Hindawi
Journal of Nanomaterials
Volume 2022, Article ID 8752664, 10 pages
https://doi.org/10.1155/2022/8752664

Research Article

Analysis of Physical, Ocular, and Aquaphobic Properties of Zirconium Oxide Nanofilms by Varying Sputtering Pressure

Sujit Kumar,[1] Vikramaditya Dave,[2] Muthamil Bala Krishnan,[3] V. Amudha,[4] S. Gomathi,[5] Sanjay Soni,[6] Syed Hamim Jeelani,[7] Ram Subbiah,[8] and Kassu Negash[9]

[1]*Department of Electrical and Electronics Engineering, Jain (Deemed-to-Be University), Bengaluru, Karnataka 560069, India*
[2]*Department of Electrical Engineering, College of Technology and Engineering, Udaipur, Rajasthan 313001, India*
[3]*Research Scholar, Department of Biomedical Engineering, SRM Institute of Science and Technology, Kattankulathur, Tamil Nadu 603203, India*
[4]*Department of Electronics and Communication Engineering, Saveetha School of Engineering, Saveetha Institute of Medical and Technical Sciences, Chennai, Tamil Nadu 602105, India*
[5]*Department of Electrical and Electronics Engineering, St. Joseph's Institute of Technology, Chennai, Tamil Nadu 600119, India*
[6]*Department of Industrial and Production Engineering, Jabalpur Engineering College, Jabalpur, Madhya Pradesh 482002, India*
[7]*Department of Civil Engineering, Koneru Lakshmaiah Education Foundation, Deemed to Be University, Andhra Pradesh 522502, India*
[8]*Department of Mechanical Engineering, Gokaraju Rangaraju Institute of Engineering and Technology, Hyderabad, Telangana 500090, India*
[9]*Department of Mechanical Engineering, Faculty of Manufacturing, Institute of Technology, Hawassa University, Hawassa, Ethiopia*

Correspondence should be addressed to Kassu Negash; kassun@hu.edu.et

Received 23 February 2022; Accepted 2 April 2022; Published 6 May 2022

Academic Editor: V. Vijayan

A thin coating of zirconium oxide (ZrO_2) is placed on outdoor high-voltage insulators to minimize air fouling. ZrO_2 thin film coatings were deposited on glass substrates using a DC sputtering (reactive magnetron) technique with sputtering pressures ranging from 5 to 25 mTorr. Characterization of the deposited films was carried out utilizing approaches such as XRD, AFM, CAG, and spectrophotometer. Following the XRD peaks, when 15 mTorr is reached, the average crystallite size increases, after which it begins to decline. The wettability of the deposited thin layer is associated with the coarseness calculated by AFM. At 15 mTorr pressure, maximum aquaphobic is achieved (107.45°). At this pressure, the transmittance and bandgap were similarly determined to be 90% and 5.43 eV, respectively.

1. Introduction

The ability of insulators to function in polluted environments is a critical aspect of the insulation of power transmission lines [1]. As a result, pollution flashover has emerged as a significant issue that electrical engineers must solve in their work. Outdoor high-voltage insulators are often made of porcelain or glass, which have been in use for more than a century [2], and have high surface energy between the atoms of the material [3, 4]. The above statement is due to the powerful electrostatic interfaces between the substance's atoms, leading to an increase in impurity buildup, which results in a deterioration of the material's dielectric characteristics and a drop in the material's dielectric constant. A further risk is that the flashover conclusion might result in a catastrophic failure of the device, mainly if a contaminated layer builds [5–7]. In addition to the wind, pollution from nearby cement facilities, industrial smoke, and coastal salt [8] are all responsible for depositing contaminants on the surfaces of the insulators. Pollutants are classified as either soluble or

insoluble particles. A leakage current flows over the insulator surface when these pollutants conduct in fog, mist, or light rain, which causes it to overheat and fail [9]. Because of the leakage current, dry spots are observed on the outer part of the insulator. Due to their insulating properties, dry areas catch fire and ignite, leading to insulator surface flashover [8, 10]. Consequently, the whole power system that was interconnected with that insulating system went down.

Water spraying insulator is an expensive but frequently necessary approach that disclosures the system operative to a potentially dangerous security state [11]. An aquaphobic coating was recommended to be applied to the surface to address these limitations. It was discovered that room temperature vulcanized (RTV) coating was the solution [12, 13]. Over the past two decades, it has been utilized to great success as an outdoor insulating material. Although it has good mechanical strength, it has poor wear and corrosion resistance due to its polymer makeup. Degradation of these coatings is significantly reduced due to this effect [14]. Recent research has focused on developing inorganic aquaphobic nanocoatings with superior mechanical, electrical, and thermal characteristics than organic coatings [15].

Zirconium oxide (ZrO_2) is a chemical compound that has applications in science and technology [16–21]. A wide variety of technical applications might benefit from ZrO_2's chemical, electrical, and mechanical properties [16–18]. However, there are no many studies that have been done on the aquaphobic behavior of ZrO_2. RF magnetron-sputtered ZrO_2 thin film was reported to have a maximum contact angle with water of 101° by Patel et al. [22]. By varying the sputtering pressure from 5 to 25 mTorr, the current work seeks to evaluate the physical, ocular, and aquaphobic characteristics of ZrO_2 surfaces, as well as their effect on surface coarseness.

Some deposition processes are employed to create ZrO_2 films, and these methods are discussed in detail in [23–31]. Each technique has its own set of benefits and drawbacks. When it comes to thin film deposition, DC reactive magnetron sputtering method stands out among the other methods because of its reproducibility, homogeneity, excellent adhesion, and convenience of usage [32, 33]. Because of this, the study concentrated on depositing thin films with varied sputtering pressures utilizing the DC reactive magnetron technique to achieve the desired results.

2. Experimentation Specifics

ZrO_2 films are generated by DC sputtering in a chamber mainly constructed for this purpose (Excel Instruments India), as shown in Figure 1. The target was made of pure zirconium metal and had a diameter of 2 inches and a thickness of 5 mm. Glass and silicon substrates were used in this experiment. After cleaning with an ultrasonic acetone solution and drying them for 2 minutes, the substrates were put on a glass substrate holder. The target-substrate distance was 41 mm in this case.

At the deposition, the chamber was expatriated with a vacuum pressure of $5 \times 10 - 6$ mTorr. With a fixed self-bias supply of 60 watt, a zirconium oxide target was sputtered in an argon-oxygen gas combination. The pure argon (Ar) and oxygen (O) gas were separately injected into the chamber. Oxygen and argon gas flow was kept constant at 10 and 40 sccm, respectively, and pressure inside the chamber varied from 5 to 25 mTorr.

The microstructure of the films was examined through a "Bruker D8 advance diffractometer with Cu-K (40 kV, 20 mA) radiation at 20°–80°." The introductory study of the deposited film was carried out with the help of an energy dispersive X-ray (EDX) connected to a scanning electron microscope (SEM) (FEI, Quanta 200 F). Analysis of the surfaces of ZrO_2 films was carried out using atomic force microscopy (AFM) in the partial-contact method. A surface profilometer was used to measure the layer thickness. Contact angle goniometry measured the water droplet contact angles. By using a UV-NIR spectrophotometer, the ocular characteristics of ZrO_2 films were investigated.

3. Results and Discussion

Various XRD patterns of nanocrystalline ZrO_2 thin films were generated under multiple pressure ranges, as seen in Figure 2. It is confirmed by the existence of a big bump at $2\theta = 31.468°$ in all deposited samples that there is a (111) plane of the monoclinic ZrO_2 structure present. This plane is indexed according to normal JCPDS (reference code: 00-037-1484) patterns for ZrO_2 lattice in all deposited samples. A less dominant peak is caused by the orientation (-111) of the monoclinic phase of ZrO_2 due to its exposure (-111).

In response to an increase in pressure (5-15 mTorr), the concentration of the emitted radiation rises (from 5 to 15 mTorr), implying a lessening in average crystallite size and, as a result, an increase in film crystallinity. In response to the rise in pressure between 15 and 25 mTorr, the (111) peak concentration declines correspondingly. The principal free path of the atoms is reduced when the deposition pressure is increased, which raises the possibility of particle collisions inside the gas environment. As a result, their kinetic energy is lowered when charged particles collide with a target surface [33–35]. Using the well-known Scherrer's formula [36], we were able to establish the average crystallite size "t."

Figure 3 depicts the variability in average crystallite size regarding pressure during the sputtering process. The connection between MFP and the atomic diameter of the gas, which may be expressed mathematically as [37], explains why the size of crystallites increases with pressure increments up to 15 mTorr.

According to the equation [37], when pressure raises from 5 to 15 mTorr, the size of crystallites increases and decreases from 15 to 25 mTorr, respectively. The mobility of crystallites explains the previous argument.

With increasing sputtering pressure, the mobility of crystallites reduces. Collisions with Ar ions diminish the amount of ejected particles that reach the surface of the substrate when the pressure is greater than 15 mTorr. Because of this, surface diffusion requires less energy. Crystallite size is reduced due to decreased surface mobility of sprayed particles [37].

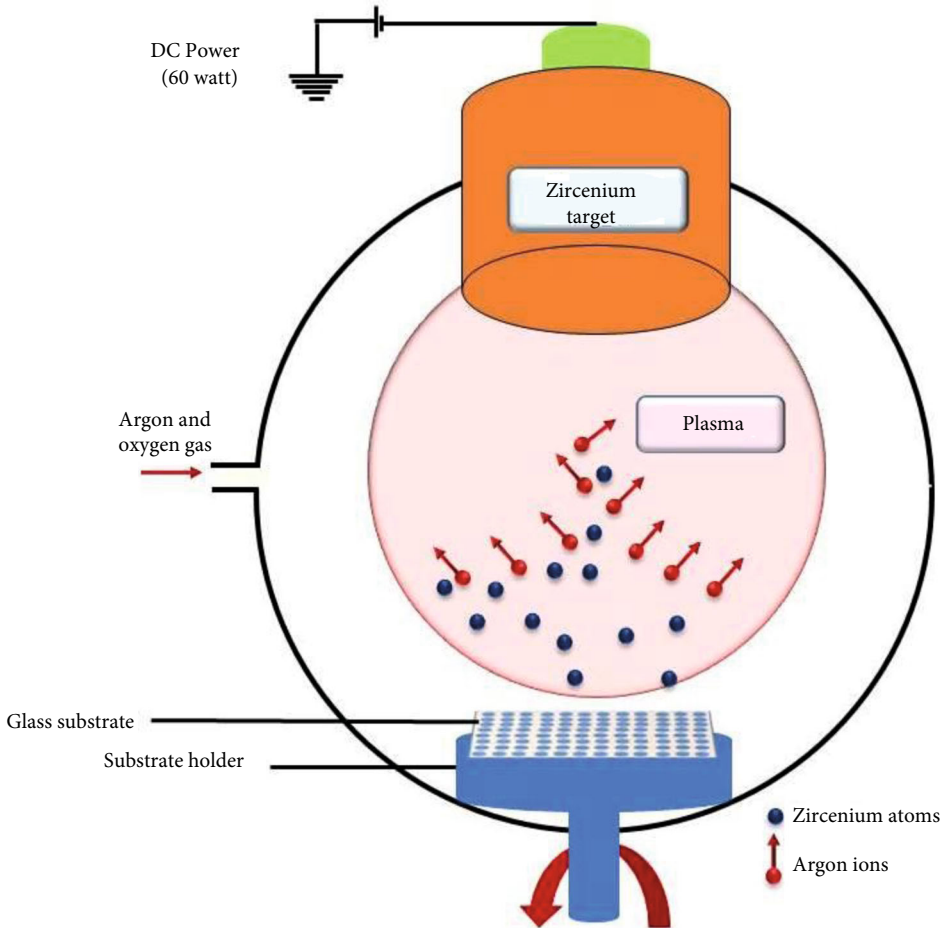

Figure 1: Schematic diagram of sputtering chamber.

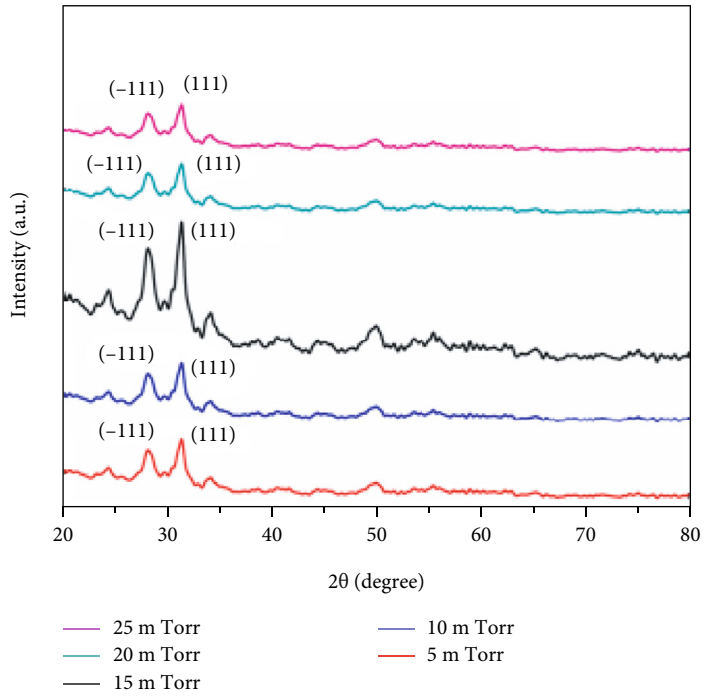

Figure 2: Intensity of deposited ZrO_2 XRD for the pressure ranges from 5 to 25 mTorr.

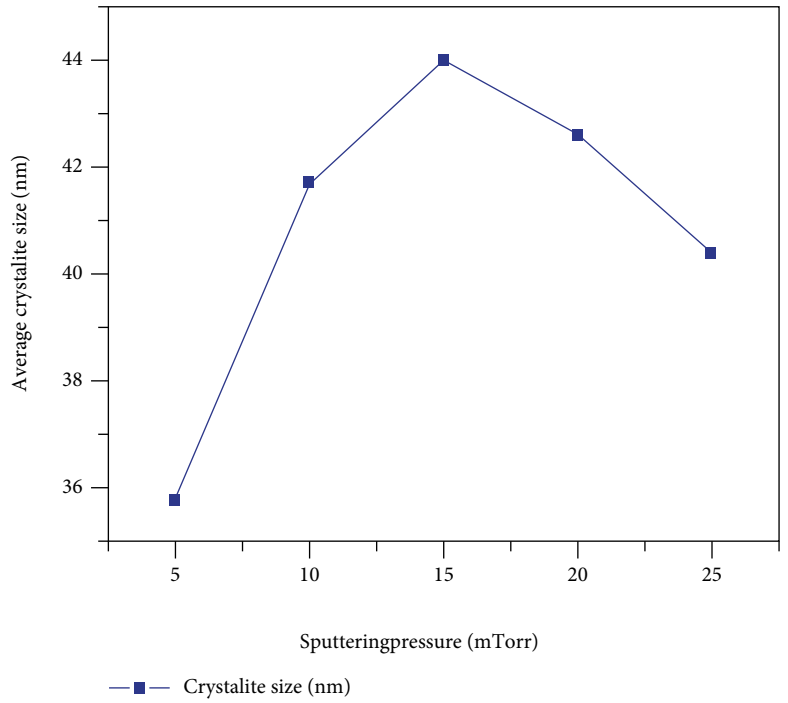

Figure 3: Average crystallite size varies with sputtering pressure.

Table 1: ZrO_2 film parameters at various pressures.

Pressure (mTorr)	O (atomic weight %)	Zr (atomic weight %)	Average transmittance %	Extinction coefficient	Bandgap (eV)
5	72.62	27.38	98	0.22	5.33
10	72.89	27.11	96	0.28	5.35
15	72.02	27.98	94	0.31	5.43
20	72.08	27.92	95	0.26	5.41
25	73.21	26.79	97	0.23	5.39

EDX was used to determine the stoichiometry of crystalline films in the laboratory. Zirconium and oxygen atomic percentages are displayed in Table 1 at various pressures. The O/Zr ratio in all of the samples was deposited at 2 : 1.

Figure 4 depicts AFM micrographs of films formed at various pressures. The AFM micrographs show that the morphologies of the ZrO_2 films are pretty similar to one another. They are all composed of spherical particles that have been roughly compacted.

Even after increasing or decreasing the pressure used in sputtering, the particle size did not remain consistent. Using data analysis techniques, the AFM evaluates the surface coarseness of thin films that have been deposited. The root mean square (RMS) technique was used to determine the surface coarseness of each ZrO_2 film sample at five different locations on its surface. Figure 5 depicts the change in RMS surface coarseness in contrast with pressure.

Initially, the coarseness increases between 5 and 15 mTorr and subsequently reduces between 15 and 25 mTorr. At 15 mTorr pressure, the surface coarseness reaches its maximum (43.5 nm). From 5 to 15 mTorr, the pressure is raised, and the size of the crystallites and the coarseness of the crystals both increase as the pressure is increased.

In response to increasing pressure (from 15 to 25 mTorr), the size of the crystallites is reduced, which results in a reduction in the coarseness of the films (from coarse to fine) [37, 38].

The aquaphobic of thin films was determined by measuring the angle they came into contact with water after being freshly formed. The contact angle was calculated using the sessile drop method. The contact angles of each sample were measured using a 3 μL drop of the solution. The contact angle variation with pressure is shown in Figure 5. The contact angle (aquaphobic) rose as the pressure climbed from 5 to 15 mTorr, reaching a maximum of 107° at 15 mTorr. In this experiment, the contact angle decreased for increasing pressure from 15 to 25 mTorr; this contact angle measures how aquaphobic the material is. It was demonstrated that aquaphobic operate similarly to coarseness, and it further clarified the influence of coarseness on contact angle (aquaphobic) [38]. As a result, the coarseness of the surface increases, which increases its aquaphobic. Wenzel has also developed the following equation [39]. According

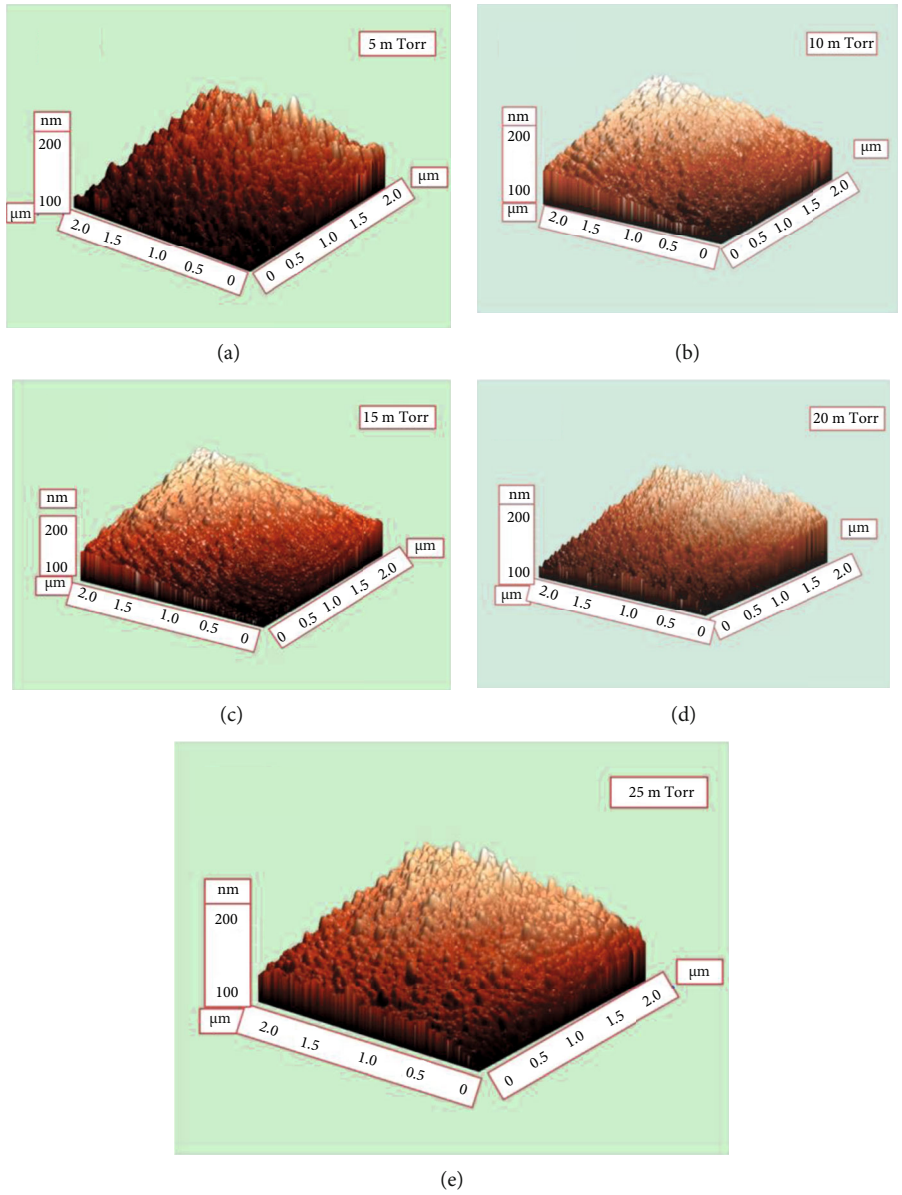

Figure 4: 3D pictures of ZrO_2 coating at numerous pressures using AFM.

to Wenzel's equation, a hydrophilic surface (<90°) grows more hydrophilic, while an aquaphobic surface (>90°) becomes more aquaphobic [40].

Figure 6 shows a plot of the transmittance band for all samples put on glass substrates in contrast with wavelength for all samples.

As a function of wavelength, the interference effect shows the oscillations in the spectrum due to the interaction. Table 1 depicts the average diffusion of each sample that has been placed. Although the intermediate diffusion level increases when the pressure exceeds 15 mTorr, the average transmission level falls when the pressure increases between 5 and 15 mTorr. Transparency and aquaphobic are inversely proportional to one another. As surface coarseness rises, so does aquaphobic, but this also results in light scattering sources [9]. As a result, the transparency of the deposited films is diminished. Even though the variation in the coarseness of deposited films was minimal (less than 1 nm), it cannot be attributed to a single reason for the significant change in limpidity (5%). Numerous elements such as the extinction coefficient and defect density may be present in this adjustment [41]. In each sample, the average transmission rate was higher than 90 percent on average. As a result, the thin coatings that are deposited are transparent while also being aquaphobic.

Using the envelope approach, the diffusion data was utilized to compute the deposited samples' refractive index (RI) [42].

Using a wavelength of 550 nm, Figure 7 depicts the change in RI of films formed under different pressures and circumstances.

In this case, the refractive index ranges between 2.19 and 2.25, comparable to the bulk value [43]. While under pressure, the refractive index lowers from 5 to 15 mTorr,

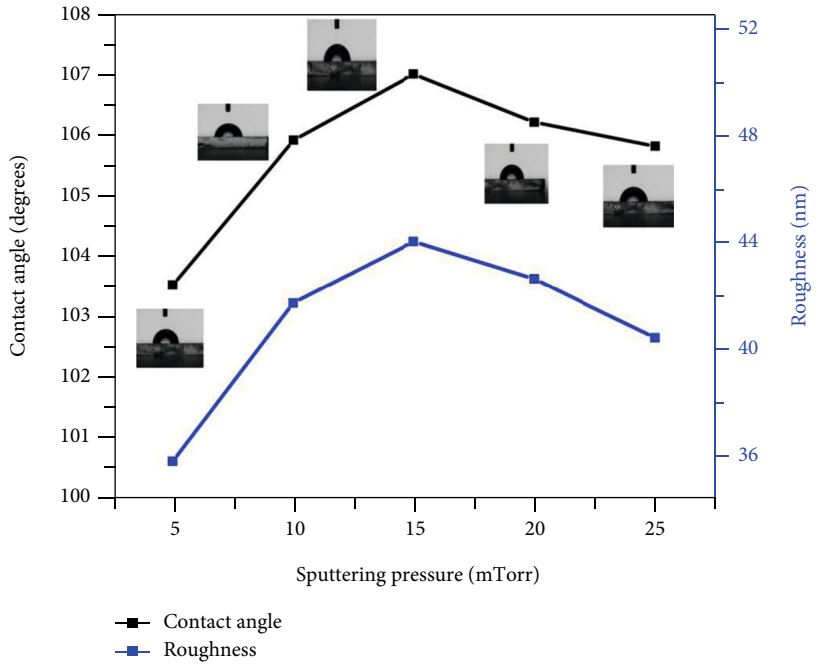

Figure 5: Contact angle and coarseness variation with sputtering pressure.

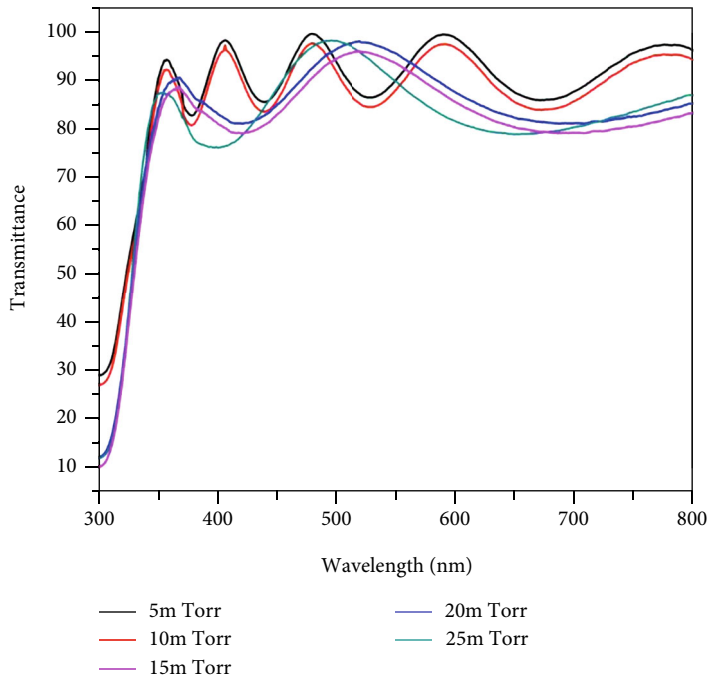

Figure 6: Ocular diffusion curve of deposited ZrO_2 thin film at varied pressures.

following which it starts to rise at 15 mTorr, and it continues to increase afterward. A variation in the transparency of the sampled film was determined to be the source of the variation in RI of ZrO_2 coating with raising sputtering pressure [44]. This change in transparency was a concerning coarseness of the sampled film. When comparing packing density to RI, the packing density of a film is highly significant [45].

The fluctuation in packing density concerning pressure is seen in Figure 7. Observation of substantial packing density in the deposited ZrO_2 thin film at 5 mTorr sputtering pressure indicated that the film had a densely packed structure.

The coating thickness was measured with the help of a surface profilometer. The diffusion statistics were too

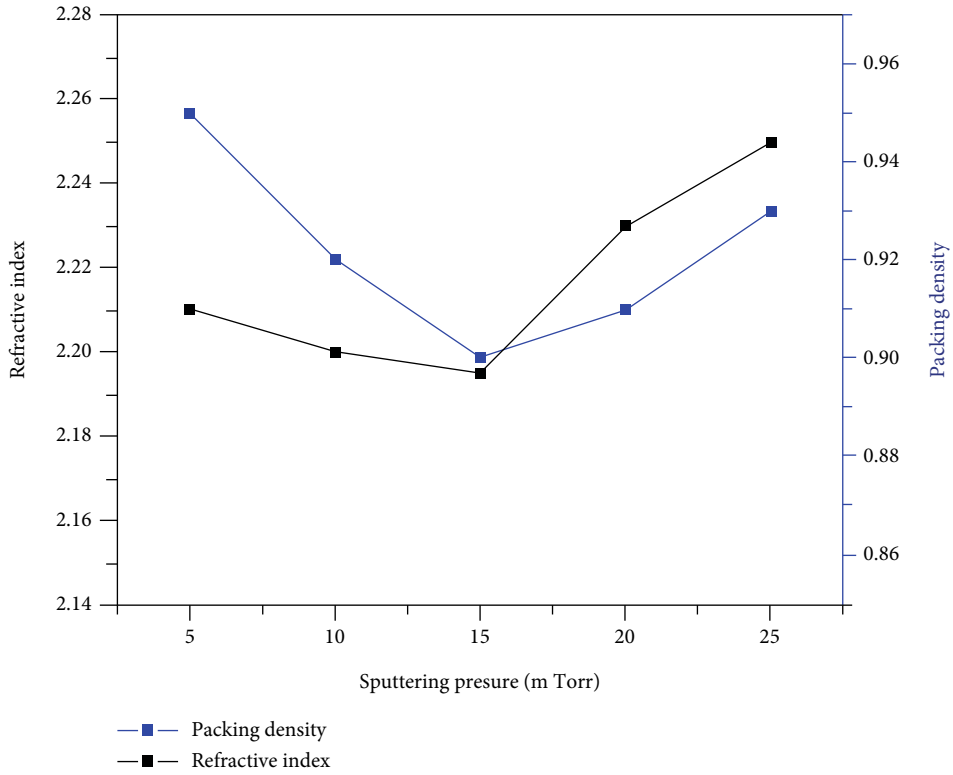

Figure 7: ZrO_2 thin film indicating RI and packing density at different pressures.

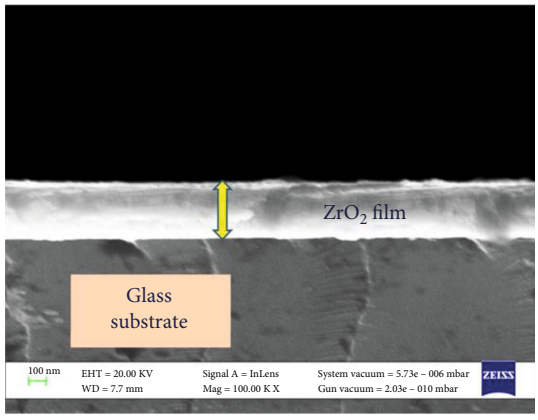

Figure 8: X-sectional SEM picture of ZrO_2 sample.

Table 2: Width of ZrO_2 films by SEM cross-section.

Pressure (mTorr)	Width of ZrO_2 films (nm)		
	SEM image	Surface profilometer	Transmission data
5	715	713	714
10	728	726	727
15	735	730	734
20	724	722	723
25	713	711	712

utilized to compute the layer width (d) using reference [40]. Using SEM cross-sectional images shown in Figure 8, the width of the film is validated even more precisely. The thickness of the films deposited using the procedures as mentioned earlier is depicted in Table 2.

It makes little difference whatever approach is employed because the breadth of each film is very near to the same. When the pressure is increased from 5 to 15 mTorr, the breadth of the ZrO_2 film grows and then begins to decrease. When particles are placed on the substrate, a loose packing arrangement results in higher film thickness for a given quantity of particles [9]. At 15 mTorr, the packing density was the highest (0.9). The maximum width (735 nm) was achieved using scanning electron microscope equipment at a pressure of 15 mTorr.

The visual immersion coefficient (α) was calculated from the relation [46]. The properties of inner reflections and typical incidence reflectance become less significant as the ocular density increases [40].

The extinction coefficient at 550 nm is seen in Table 1. The k value increases from 5 to 15 mTorr and then falls. Changes in film transparency are driven mainly by variations in the extinguishment coefficient. The extinction coefficient of deposited films is affected by the dispersion of the grains. A film's transparency decreases with increasing grain size because the impact of scattering increases with increasing grain size [47]. Pressure is raised from 5 to 15 mTorr, and the k value rises (0.22 to 0.31), resulting in a fall in average transparency from 97 to 90% when the pressure is increased. The increased pressure of more than

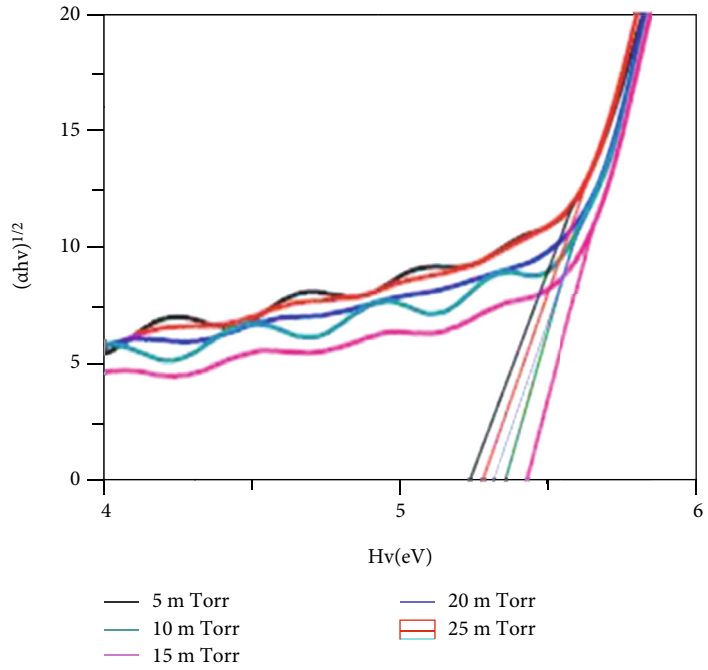

Figure 9: Ocular bandgap of ZrO_2 film at various sputtering pressure.

15 mTorr decreases grain size and boosts film transparency from 90 to 95%.

A thin layer of nanocrystalline zirconium oxide was investigated for its visual bandgap (Eg), which was calculated from immersion coefficient (α) employing the Tauc relation [48]. The value of n was set to 1/2 [48] for transitions that were permitted directly. The ocular bandgap may be calculated from a graph of $(\alpha h\nu)^{1/2}$ vs $h\nu$. Figure 9 shows the relationship between $(\alpha h\nu)^{1/2}$ and photon energy $h\nu$ for samples placed at various pressures.

Table 1 displays the bandgap values that were calculated at various pressures. The bandgap of ZrO_2 film produced varies between 5.23 and 5.43 eV, which is equivalent to the bandgap of ZrO_2 in bulk [49]. The largest bandgap (5.43 eV) was discovered at a pressure of 15 mTorr. ZrO_2 thin films have a bandgap that increases between 5 and 15 mTorr and decreases after 15 mTorr. The size of the crystallites affects the bandgap [48], and the size of crystallites explains the phenomenon described in [48].

4. Conclusions

The physical, optical, and aquaphobic properties of nanostructured ZrO_2 nanofilms were investigated on glass samples at various pressures and temperatures. A 15 mTorr pressure resulted in a monoclinic structure that was strongly oriented (111). The main objective of the work was to achieve a high aquaphobic coating (107°) with a large bandgap (5.43 eV) and a thin film (735 nm) using high sputtering pressure of 15 mTorr while using a thin film sputtering technique. On the other hand, the decreased sputtering pressure reduces transparency and refractive index, which might be missed owing to the enhanced aquaphobic of the material. The optimum sputtering pressure for generating dielectric aquaphobic coatings for outdoor insulators was 15 mTorr, which was shown to be the case in this study. Additionally, when compared to HfO_2 coating over a glass substrate, ZrO_2 was shown to be the superlative coating since its aquaphobic was higher than that of HfO_2.

Data Availability

The data used to support the findings of this study are included in the article. Should further data or information be required, these are available from the corresponding author upon request.

Disclosure

This study was performed as a part of the Employment Hawassa University, Ethiopia.

Conflicts of Interest

The authors declare that there are no conflicts of interest regarding the publication of this paper.

Acknowledgments

The authors appreciate the technical assistance to complete this experimental work from Department of Mechanical Engineering, St. Joseph's Institute of Technology, Chennai, Tamil Nadu, India. The authors are thankful for the technical assistance to complete this experimental work.

References

[1] N. Dhahbi-Megriche, A. Beroual, and L. Krahenbuhl, "A new proposal model for flashover of polluted insulators," *Journal of Physics D: Applied Physics*, vol. 30, no. 5, pp. 889–894, 1997.

[2] R. Hackam, "Outdoor HV composite polymeric insulators," *IEEE Transactions on Dielectrics and Electrical Insulation*, vol. 6, no. 5, pp. 557–585, 1999.

[3] H. Deng, R. Hackam, and E. A. Cherney, "Influence of thickness, substrate type, amount of silicone fluid and solvent type on the electrical performance of RTV silicone rubber coatings," *Power Delivery*, vol. 11, no. 1, pp. 431–443, 1996.

[4] R. S. Gorur, E. A. Chernry, and J. T. Burnham, *Outdoor Insulators*, Arizona, USA, Phoenix, 1st edn edition, 1999.

[5] H. Su, Z. Jia, Z. Guan, and L. Li, "Mechanism of contaminant accumulation and flashover of insulator in heavily polluted coastal area," *IEEE Transactions on Dielectrics and Electrical Insulation*, vol. 17, no. 5, pp. 1635–1641, 2010.

[6] B. S. Reddy and G. R. Nagabhushana, "Study of temperature distribution along an artificially polluted insulator String," *Plasma Science and Technology*, vol. 5, no. 2, pp. 1715–1720, 2003.

[7] M. Farzaneh and J. F. Draupeau, "AC flashover performance of insulators covered with artificial ice," *Power Delivery*, vol. 10, no. 2, pp. 1038–1051, 1995.

[8] P. J. Lambeth, "Effect of pollution on high voltage insulators proc," *IEE Review*, vol. 118, pp. 1107–1114, 1971.

[9] S. Jain, A. Sanger, and R. Chandra, "Sputtering pressure dependent structural, optical and aquaphobic properties of DC sputtered Pd/WO3 thin films for hydrogen sensing application," *Emerging Energy Technology perspectives-A Sustainable Approach*, vol. 549, pp. 146–154, 2014.

[10] G. M. Tena, R. H. Corona, and I. R. Vazquez, "Experiences on pollution level measurement in Mexico," *Electric Power Systems Research*, vol. 76, no. 1-3, pp. 58–66, 2005.

[11] K. F. Portella, F. Piazza, P. C. Inone et al., "Efeitos da poluição atmosférica (litorânea e industrial) em isoladores da rede elétrica da região metropolitana de Salvador," *Química Nova*, vol. 31, no. 2, pp. 340–348, 2008.

[12] S. M. Gubanski, "Properties of silicone rubber housings and coatings," *IEEE Transactions on Electrical Insulation*, vol. 27, no. 2, pp. 374–382, 1992.

[13] G. G. Karady, "Flashover mechanism of non-ceramic insulators," *IEEE Transactions on Dielectrics and Electrical Insulation*, vol. 6, no. 5, pp. 718–723, 1999.

[14] D. Devendranath and A. D. Rajkumar, "Leakage current and charge in RTV coated insulators under pollution conditions," *IEEE Transactions on Dielectrics and Electrical Insulation*, vol. 2, pp. 294–301, 2002.

[15] Y. Cao, P. C. Irwin, and K. Younsi, "The future of nanodielectrics in the electrical power industry," *IEEE Transactions on Dielectrics and Electrical Insulation*, vol. 11, no. 5, pp. 797–807, 2004.

[16] M. L. Green, E. P. Gusev, R. Degraeve, and E. L. Garfunkel, "Ultrathin (<4 nm) SiO2 and Si-O-N gate dielectric layers for silicon microelectronics: understanding the processing, structure, and physical and electrical limits," *Journal of Applied Physics*, vol. 90, no. 5, pp. 2057–2121, 2001.

[17] D. Chi and P. C. McIntyre, "Germanium n-type shallow junction activation dependences," *Applied Physics Letters*, vol. 88, pp. 232901–232907, 2005.

[18] C. M. Wang, S. Azad, S. Thevuthasan, V. Shutthanandan, D. E. Mc-Cready, and C. H. F. Peden, "Spectroscopic ellipsometry characterization of the optical properties and thermal stability of ZrO_2 films made by ion-beam assisted deposition," *Journal of Materials Research*, vol. 19, pp. 1315–1322, 2008.

[19] W. L. Gong, W. Lutze, and R. C. Ewing, "Zirconia ceramics for excess weapons plutonium waste," *Journal of Nuclear Materials*, vol. 277, no. 2-3, pp. 239–249, 2000.

[20] S. Venkataraj, O. Kappertz, R. Jayavel, and M. Wuttig, "Growth and characterization of zirconium oxynitride films prepared by reactive direct current magnetron sputtering," *Journal of Applied Physics*, vol. 92, no. 5, pp. 2461–2466, 2002.

[21] S. Ramanathan and P. C. Mclntyre, "Ultrathin zirconia/SiO2-dielectric stacks grown by ultraviolet–ozone oxidation," *Applied Physics Letters*, vol. 80, no. 20, pp. 3793–3795, 2002.

[22] U. S. Patel, K. H. Patel, K. V. Chauhan, A. K. Chawla, and S. K. Rawal, "Investigation of various properties for zirconium oxide films synthesized by sputtering," *Procedia Technology*, vol. 23, pp. 336–343, 2016.

[23] S. Harasek, A. Lugstein, H. D. Wanzenboeck, and E. Bertagnolli, "Slow trap response of zirconium dioxide thin films on silicon," *Applied Physics Letters*, vol. 83, no. 7, pp. 1400–1402, 2003.

[24] R. Puthenkovilakam and J. P. Chang, "Valence band structure and band alignment at the ZrO_2/Si Interface," *Applied Physics Letters*, vol. 84, no. 8, pp. 1353–1355, 2004.

[25] A. Stesmans and V. V. Afanas'ev, "Si dangling-bond-type defects at the interface of (100)Si with ultrathin layers of SiOx, $Al2O_3$, and ZrO_2," *Applied Physics Letters*, vol. 80, no. 11, pp. 1957–1959, 2002.

[26] T. Sikola, J. Spousta, L. Dittrichova, and L. Benes, "Deposition of magnetic thin films by IBAD," *Nuclear Instruments and Methods in Physics Research Section B: Beam Interactions with Materials and Atoms*, vol. 148, no. 1-4, pp. 907–911, 1999.

[27] A. Meher, H. Klumper-Westkamp, F. Hoffmann, and P. Mayr, "Crystallization and residual stress formation of sol-gel-derived zirconia films," *Thin Solid Films*, vol. 308-309, pp. 363–368, 1997.

[28] S. Kumar, K. Vikramaditya Dave, V. Velmurugan et al., "Analysis of structural, optical, and aquaphobic properties of zirconium oxide nanofilms by varying sputtering gas," *Advances in Materials Science and Engineering*, vol. 2022, Article ID 9968485, 2022.

[29] J. M. Howard, V. Craciun, C. Essary, and R. K. Singh, "Interfacial layer formation during high-temperature annealing of ZrO_2 thin films on Si," *Applied Physics Letters*, vol. 81, no. 18, pp. 3431–3433, 2002.

[30] J. S. Kim, H. A. Marzouk, and P. J. Reucroft, "Deposition and structural characterization of ZrO_2 and yttria-stabilized ZrO_2 films by chemical vapor deposition," *Thin Solid Films*, vol. 254, no. 1-2, pp. 33–38, 1995.

[31] D. Ronnow, J. Isidorsson, and G. A. Niklasson, "Surface roughness of sputteredZrO2films studied by atomic force microscopy and spectroscopic light scattering," *Physical Review E*, vol. 54, no. 4, pp. 4021–4028, 1996.

[32] M. Ohring, *The Materials Science of Thin Films*, Academic Press, San Diego, 1992.

[33] T. Kamohara, M. Akiyama, N. Ueno et al., "Influence of sputtering pressure on polarity distribution of aluminum nitride, thin films," *Applied Physics Letters*, vol. 89, no. 24, article 243507, 2006.

[34] A. Ababneh, U. Schmid, J. Hernando, J. L. Sánchez-Rojas, and H. Seidel, "The influence of sputter deposition parameters on piezoelectric and mechanical properties of AlN thin films," *Materials Science and Engineering B*, vol. 172, no. 3, pp. 253–258, 2010.

[35] X.-P. Kuang, H.-Y. Zhang, G.-G. Wang et al., "AlN films prepared on 6H-SiC substrates under various sputtering pressures by RF reactive magnetron sputtering," *Applied Surface Science*, vol. 263, pp. 62–68, 2012.

[36] B. D. Cullity, *Elements of X-Ray Diffraction*, Addison-Wesley, London, 2nd edn edition, 1978.

[37] R. Vipin Chawla and R. C. Jayaganthan, "Influence of sputtering pressure on the structure and mechanical properties of nanocomposite Ti-Si-N thin films," *Journal of Materials Science and Technology*, vol. 26, no. 8, pp. 673–678, 2010.

[38] A. B. Cassie and S. Baxter, "Wettability of porous surfaces," *Transactions of the Faraday Society*, vol. 40, pp. 546–551, 1944.

[39] R. N. Wenzel, "Resistance of solid surfaces to wetting by water," *Industrial and Engineering Chemistry*, vol. 28, no. 8, pp. 988–994, 1936.

[40] K. R. Wu, J. J. Wang, W. C. Liu, Z. S. Chen, and J. K. Wu, "Deposition of graded TiO_2 films featured both hydrophobic and photo-induced hydrophilic properties," *Applied Surface Science*, vol. 252, no. 16, pp. 5829–5838, 2006.

[41] H. N. Shah, R. Vipin Chawla, and D. K. Jayaganthan, "Microstructural characterizations and hardness evaluation of d.c. reactive magnetron sputtered CrN thin films on stainless steel substrate," *Bulletin of Materials Science*, vol. 33, no. 2, pp. 103–110, 2010.

[42] J. C. Manifacier, J. Gasiot, and J. P. Fillard, "A simple method for the determination of the optical constants n, k and the thickness of a weakly absorbing thin film," *Journal of Physics E: Scientific Instruments*, vol. 9, no. 11, pp. 1002–1004, 1976.

[43] M. Jerman, Z. Qiao, and D. Mergel, "Refractive index of thin films of SiO_2, ZrO_2, and HfO_2 as a function of the films mass density," *Applied Optics*, vol. 44, no. 15, pp. 3006–3012, 2005.

[44] L. Zhang, D. Ouyang, and C. Mo, "Characterizations of optical absorption in porous Al_2O_3 ☒Cr_2O_3 nanocomposites," *Nanostructured Materials*, vol. 9, no. 1-8, pp. 563–566, 1997.

[45] G. Bauer, "Absolutwerte der optischen Absorptionskonstanten von Alkalihalogenidkristallen im Gebiet ihrer ultravioletten Eigenfrequenzen," *Annalen der Physik*, vol. 411, no. 4, pp. 434–464, 1934.

[46] Z. S. El Mandouh and M. S. Selim, "Physical properties of vanadium pentoxide sol gel films," *Thin Solid Films*, vol. 371, pp. 59–64, 2000.

[47] G. He, L. Q. Zhu, M. Liu, Q. Fang, and L. D. Zhang, "Optical and electrical properties of plasma-oxidation derived HfO_2 gate dielectric films," *Applied Surface Science*, vol. 253, no. 7, pp. 3413–3418, 2007.

[48] C. V. Ramana, R. S. Vemuri, I. Fernandez, and A. L. Campbell, "Size-effects on the optical properties of zirconium oxide thin films," *Applied Physics Letters*, vol. 95, no. 23, pp. 231905–231912, 2009.

[49] J. G. Bendoraitis and R. E. Salomon, "Optical energy gaps in the monoclinic oxides of hafnium and zirconium and their solid Solutions[1]," *The Journal of Physical Chemistry*, vol. 69, no. 10, pp. 3666-3667, 1965.